

Magnetic order and the electronic ground state in the pyrochlore iridate $\text{Nd}_2\text{Ir}_2\text{O}_7$

Authors: Steven M. Disseler, Chetan Dhital, Thomas C. Hogan, A. Amato, S. R. Giblin, Clarina de la Cruz, A. Daoud-Aladine, Stephen Wilson, Michael J. Graf

Persistent link: <http://hdl.handle.net/2345/3688>

This work is posted on [eScholarship@BC](#),
Boston College University Libraries.

Published in *Physical Review B*, vol. 85, no. 17, May 2012

Copyright (2012) by The American Physical Society. These materials are made available for use in research, teaching and private study, pursuant to U.S. Copyright Law. The user must assume full responsibility for any use of the materials, including but not limited to, infringement of copyright and publication rights of reproduced materials. Any materials used for academic research or otherwise should be fully credited with the source.

Magnetic order and the electronic ground state in the pyrochlore iridate Nd₂Ir₂O₇S. M. Disseler,¹ Chetan Dhital,¹ T. C. Hogan,¹ A. Amato,² S. R. Giblin,³ Clarina de la Cruz,⁴ A. Daoud-Aladine,³ Stephen D. Wilson,¹ and M. J. Graf¹¹*Department of Physics, Boston College, Chestnut Hill, Massachusetts 02467, USA*²*Paul Scherrer Institute, CH 5232 Villigen PSI, Switzerland*³*Rutherford Appleton Laboratory, Didcot, Oxfordshire OX11 0QX, UK*⁴*Quantum Condensed Matter Division, Oak Ridge National Laboratory, Oak Ridge, Tennessee 37831-6393, USA*

(Received 29 January 2012; published 31 May 2012)

We report a muon spin relaxation/rotation, bulk magnetization, neutron scattering, and transport study of the electronic properties of Nd₂Ir₂O₇. We observe the onset of strongly hysteretic behavior in the temperature-dependent magnetization below 120 K, and an abrupt increase in the temperature-dependent resistivity below 8 K. Muon spin relaxation measurements show that the hysteretic magnetization is driven by a transition to a magnetically disordered state, and below 8 K a magnetically ordered ground state sets in, as evidenced by the onset of spontaneous muon precession. Our measurements point toward the absence of a true metal-to-insulator phase transition in this material and suggest that Nd₂Ir₂O₇ may lie within or on the metallic side of the boundary of the Dirac semimetal regime within its topological phase diagram.

DOI: [10.1103/PhysRevB.85.174441](https://doi.org/10.1103/PhysRevB.85.174441)

PACS number(s): 75.30.-m, 76.75.+i, 75.47.Lx

Correlated iridium oxide compounds have attracted a great deal of interest due to the delicate interplay between electron-electron correlation effects and spin-orbit induced band renormalization manifest in these materials,¹⁻³ and a number of novel topological phase transitions have been proposed as the correlations in these systems are tuned from strongly correlated Mott insulators to weakly correlated topological band insulators. The most striking of these is the Dirac semimetal phase, which is predicted to possess topologically protected electronic states along only particular momentum points and crystallographic surfaces in a three-dimensional solid with magnetic correlations.²

The most promising iridates for exploring this topological phase diagram are currently the A₂Ir₂O₇ (A-227) pyrochlore compounds where, through tuning the A site, the system transitions from magnetically ordered^{4,5} insulators^{6,7} into a spin-disordered,⁸ unconventional metal.⁹ Near the transition from the Mott insulating phase to the metallic ground state within the topological phase diagram, the topologically nontrivial Dirac semimetallic phase is predicted to emerge,² and such a transition likely occurs between the known correlated insulating phase of Eu₂Ir₂O₇^{6,7} and the unconventional metallic phase of Pr₂Ir₂O₇.⁹ The insulating A-227 materials all display metal-to-insulator (MI) phase transitions at their respective Ir⁴⁺ ordering temperatures; however Nd₂Ir₂O₇ (Nd-227) shows a dramatically reduced MI transition onset temperature.^{10,11} This supports a picture of Nd-227 residing just inside the correlated, insulating boundary of the Dirac semimetal phase transition line. Studies of the intrinsic behavior of the Nd-227 ground state are thus an important metric for exploring Nd-227's capacity for being tuned into novel ground states.

Conflicting experimental reports have revealed a complex picture of the intrinsic Nd-227 electronic ground state, suggesting that the reported insulating phase in this material is a delicate balance between sample stoichiometry and other extrinsic factors. Initial reports showed Nd-227 was clearly metallic at all temperatures,⁶ whereas in later studies a MI transition was reported at 37 K.¹⁰ Subsequent studies of the

resistivity under pressure¹¹ revealed a small upturn in the resistivity below 20 K—interpreted as the MI transition—which was suppressed under an increased pressure of 10 GPa. At these higher pressures, a small resistive anomaly was observed near $T = 3.3$ K that was associated with the onset of magnetic order via an RKKY interaction facilitated by the suppression of the MI transition. Recent studies support the idea of a high sensitivity of the properties of the pyrochlore iridates to chemical stoichiometry.¹²

The magnetic order associated with this upturn in resistivity was initially presumed to be ferromagnetic based on the detailed magnetic response of the resistivity, with a 2-in/2-out structure of the Nd³⁺ ($J = 9/2$) moments. Recent neutron scattering measurements, however, suggest that magnetic ordering of the Ir⁴⁺ moments occurs at ambient pressure below 15 K¹³ in a structure consistent with an all-in/all-out arrangement. The large decoupling between the reported MI transition temperature ($T \sim 37$ K) and onset of correlated magnetism is strongly suggestive of additional interactions relevant to the ground state.

In order to explore the interactions between the correlated spin order and the charge carriers in this material, we present a magnetization, transport, neutron diffraction, and muon spin relaxation/rotation (μ SR) study on polycrystalline samples of Nd-227. We find the onset of a disordered magnetic state at 120 K associated with the Ir⁴⁺ sublattice. Upon continued cooling below 8 K, we observe the onset of long-range magnetic order likely associated with the Ir⁴⁺ sublattice. Our combined results find no evidence for a metal-to-insulator transition in this system, suggesting that the Nd-227 system may already lie just within the metallic regime, bridging the gap between the magnetically ordered insulating and disordered metallic phases.

Polycrystalline samples of Nd₂Ir₂O₇ were synthesized by reacting stoichiometric amounts of Nd₂O₃ (99.99%) and IrO₂ (99.9%) in air to minimize variations in the oxygen stoichiometry. Powders were pelletized using an isostatic cold press and reacted between 900 °C and 1125 °C over six days with several intermediate grindings. The samples were

determined to be phase pure with the exception of two minor impurity phases of IrO_2 and Nd_2O_3 each comprising less than 1% of the total volume fraction. Powder x-ray diffraction measurements yielded narrow line shapes comparable to the best previously reported data on Nd-227, demonstrating the high homogeneity of the sample stoichiometry.¹⁰

Neutron experiments were performed on the HB-2A powder diffractometer at the High Flux Isotope Reactor at Oak Ridge National Lab and on the HRPD instrument at the ISIS spallation neutron facility. Magnetization measurements were performed in an Oxford MagLab dc-extraction magnetometer. The electrical resistivity was measured using standard ac four-probe techniques in gas flow and ^3He cryostats with a 9 T magnet. Magnetic fields were applied parallel to the current, and the excitation level was varied to ensure no self-heating occurred. Muon spin relaxation (μSR) measurements were carried out over the temperature range $1.6\text{ K} < T < 150\text{ K}$ on the EMU spectrometer at the ISIS facility at the Rutherford Appleton Laboratories and the GPS spectrometer on the πM3 beamline at the Paul Scherrer Institute (PSI). Powder samples were studied at ISIS in a silver holder with a Mylar window, and the small contribution (10%) of muons stopping in the silver was independently measured and subtracted from the data. Powder samples at PSI were sealed in metalized Mylar packets, with no background contribution.

The temperature-dependent static susceptibility $\chi(T) = M/H$ of polycrystalline was measured from 250 K to 1.8 K in a field of 1000 Oe under both zero-field-cooled (ZFC) and field-cooled (FC) conditions [Fig. 1(a)]. Under ZFC

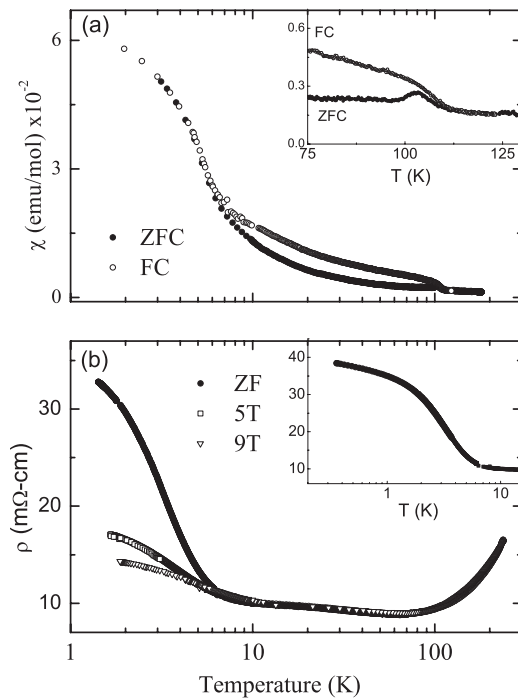


FIG. 1. (a) Magnetization versus temperature in 1000 G for field-cooled (solid symbols) and zero-field-cooled (open symbols) sample of $\text{Nd}_2\text{Ir}_2\text{O}_7$. Inset: Expanded view of the susceptibility in the vicinity of $T = 120\text{ K}$. (b) Resistivity versus temperature for $\text{Nd}_2\text{Ir}_2\text{O}_7$ in applied fields of 0 T, 5 T, and 9 T. Inset: Temperature-dependent resistivity at low temperatures in zero applied field.

conditions, we observe a small peak in Nd-227 at 105 K, while under FC conditions we see a sharp increase at $T = 120\text{ K}$, similar to that observed for other members of the A-227 family at comparable temperatures.^{6,7} It is associated with the onset of magnetism in the Ir^{4+} sublattice, as it occurs when the A-site species is either magnetic or nonmagnetic. The anomaly is typically linked to a MI transition, which occurs at comparable temperatures. We find however that the onset temperature of the magnetic anomaly is considerably higher than the value of $T_{\text{MI}} = 37\text{ K}$ extracted from earlier resistivity measurements.¹⁰ Cooling below 100 K there is a significant difference between the FC and ZFC behavior until 8 K, below which the ZFC and FC curves converge and continue to increase weakly with a further decrease in temperature.

The temperature-dependent resistivity of Nd-227 is shown in Fig. 1(b). A decrease in the resistivity is observed below room temperature and reaches a broad minimum at $T \sim 65\text{ K}$. Between 65 K and 8 K there is a very weak increase in the resistivity; however below 8 K there is a second slope change followed by a slow, nearly logarithmic increase in resistance with decreasing temperature [inset of Fig. 1(b)] below 1 K. This logarithmic temperature dependence differs greatly from the exponential behavior expected for an insulating state, but is characteristic of correlations in a weakly metallic system (e.g., Kondo effect); we conclude that there is no metal-insulator transition. An applied magnetic field of 9 T above 8 K has very little effect on the resistance, in contrast to the large negative magnetoresistance observed at lower temperatures. Samples from two different batches were measured, including one sample before and after a 24 hour anneal in an oxygen environment, and in all cases the data were the same, demonstrating that the observed behavior is insensitive to small changes in chemical composition.

In Fig. 2 we show the magnetic field dependence at $T = 1.8\text{ K}$ of both the magnetization and resistivity. The $J = 9/2$ state is known to split into five Kramers doublets assuming a trigonal symmetry.¹⁴ A Brillouin function with $J_{\text{eff}} = 1/2$ was used to describe the magnetization data (dashed curve in Fig. 2), for which we find an effective moment $\mu_{\text{eff}} = 1.3 \pm 0.1\ \mu_B$. This value is larger than the maximum estimated size of the Ir^{4+} moment but smaller than the free Nd^{3+} moment;

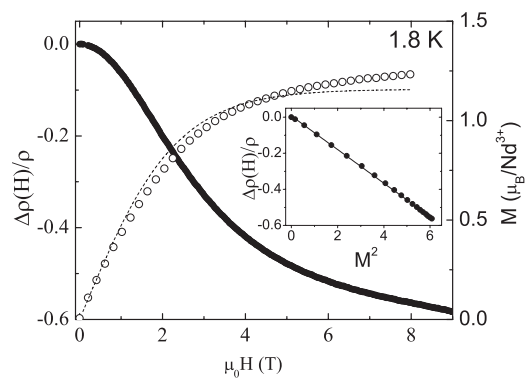


FIG. 2. Magnetic field dependence of the resistivity and magnetization at $T = 1.8\text{ K}$. The dashed line shows the fit to a Brillouin function (see text). Inset: Variation of the fractional change in resistivity with the square of the magnetization; the straight line is a guide to the eye.

thus we conclude that the Nd moments remain paramagnetic down to at least 1.8 K.

Diffraction patterns from elastic neutron scattering were refined using the Fd-3m cubic space group, and the lattice parameters were determined to be $a = 10.3588(4)$ Å at 4 K and $a = 10.3647(9)$ Å at 200 K. However, our measurements did not show any evidence of long-range magnetic order down to 4 K with the upper bound of an ordered moment conservatively estimated to be $0.5 \mu_B$. We also performed high-resolution time-of-flight diffraction measurements on HRPD at ISIS on this same sample in order to improve the statistical significance of this result. From these combined measurements, we can conclude that within comparable statistical confidence of Ref. 13 the long-range magnetic signal reported below 15 K in earlier reports is not present in our sample.¹⁵

μ SR measurements were performed on two spectrometers with complementary resolutions/sensitivities to both fast (GPS at PSI) and slow relaxation processes (EMU at ISIS). In modeling the data at higher temperatures ($T \geq 8$ K), the time-dependent depolarization curves can be fitted by a stretched exponential function

$$P(t) = A_S \exp[-(\lambda_S t)^\beta], \quad (1)$$

where A_S is the asymmetry of the depolarization, λ_S is the slow depolarization rate, and β is the stretched exponent. For the ISIS data, A_S and λ_S are both left as fit parameters, since the onset of fast depolarization will be manifest in a loss of apparent asymmetry. For the GPS data, the asymmetry was independently measured and A_S was fixed at this value. Shown in Fig. 3, above 10 K we see excellent agreement between the results taken at the two different facilities. λ_S shows a clear change at 120 K, close to the temperature at which the magnetization exhibits the onset of hysteretic behavior. Below 10 K, a dramatic increase in the relaxation rate is observed, corresponding to a rapid drop in A_S in data from EMU, reaching a value of approximately 0.39(1) of the full asymmetry at 1.6 K. This clearly demonstrates the onset of fast depolarization processes and accounts for the difference in λ_S for the two data sets below 10 K. The exponent β is shown in the inset of Fig. 3 for both the GPS and EMU. For both spectrometers β is 1.05 ± 0.02 at high temperatures. In Fig. 4,

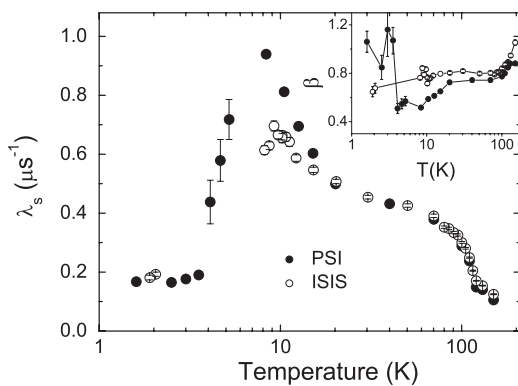


FIG. 3. Temperature-dependent muon depolarization rate extracted from data taken at ISIS and PSI, as described in the text. Inset: Temperature dependence of the stretching exponent β as described in the text.

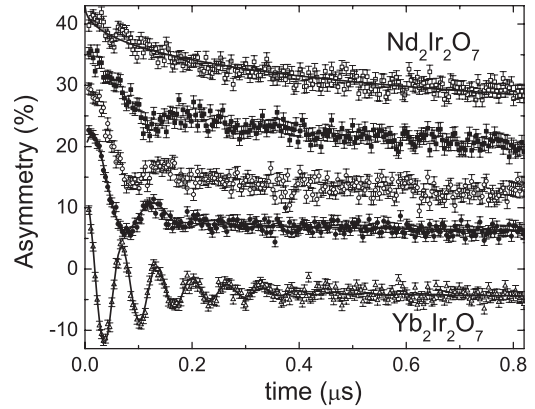


FIG. 4. Evolution of the short-time muon depolarization curves (PSI) with decreasing temperature. The upper four curves (top to bottom) are for $\text{Nd}_2\text{Ir}_2\text{O}_7$, at temperatures of 8 K, 5 K, 3.5 K, and 1.6 K; curves have been offset from the 1.6 K curve by successive increments of 6 for clarity. The bottom curve is for $\text{Yb}_2\text{Ir}_2\text{O}_7$ at 1.6 K (Ref. 5) and is offset by -12 . The solid lines are fits to Eq. (1) for the $T = 8$ K data and to Eq. (2) for the $T = 1.6$ K data for the $\text{Nd}_2\text{Ir}_2\text{O}_7$ curves; the solid line for the Yb curve is a fit described in Ref. 5.

we show a sequence of low-temperature depolarization curves taken on GPS. Upon cooling below $T = 8$ K, we see the onset of spontaneous oscillations, unambiguously demonstrating the existence of long-range magnetic order. The oscillations are heavily damped, and attempts to fit the data to the expected two-component depolarization function for polycrystalline samples with magnetic order (Refs. 4 and 5) were unsuccessful. A three-component depolarization function of the form

$$P(t) = A_1 \exp(-\lambda_1 t) \cos(\omega_\mu t + \phi) + A_2 \exp(-\lambda_2 t) + A_S \exp[-(\lambda_S t)^\beta] \quad (2)$$

yields an adequate fit to the data at $T = 1.6$ K, as shown in Fig. 4. We find a muon precession frequency $\omega_\mu/2\pi = 8.8(2)$ MHz, corresponding to an average local field of $\langle B_{\text{loc}} \rangle = \omega_\mu/\gamma_\mu = 665$ G, where γ_μ is the muon gyromagnetic ratio and $\gamma_\mu/2\pi = 0.01355$ MHz/G. The extracted frequency is significantly smaller than the 13.3 MHz value observed for $\text{Eu}_2\text{Ir}_2\text{O}_7$ ($\langle B_{\text{loc}} \rangle = 987$ G)⁴ and the 14.8 MHz ($\langle B_{\text{loc}} \rangle = 1100$ G) found for $\text{Y}_2\text{Ir}_2\text{O}_7$ and $\text{Yb}_2\text{Ir}_2\text{O}_7$ ⁵ as seen when comparing the $T = 1.6$ K depolarization curves for Nd-227 and Yb-227⁵ in Fig. 4. The depolarization rates are $\lambda_1 = 13(1) \mu\text{s}^{-1}$, $\lambda_2 = 15(2) \mu\text{s}^{-1}$, $\lambda_S = 0.18(1) \mu\text{s}^{-1}$, and $\beta = 1.07(6)$; the relative amplitudes are $A_1 = 9.3$, $A_2 = 6.7(6)$, and $A_S = 7.1(4)$; the total amplitude $A_1 + A_2 + A_S$ was constrained to be the measured full asymmetry, with the ratio of slowly decaying asymmetry to the total asymmetry, $\eta \equiv A_S/A_T$, found to be approximately 0.30(2). However, the resultant phase angle is unphysically large, $\phi = -63^\circ$, and the fit deviates from the data at very short times. So, while the fit allows us to reasonably estimate the local field and extract the rate of the slow depolarization term below 8 K [also shown in Fig. 3 for Eq. (2)], it should be treated as phenomenological.

Longitudinal field studies (see Supplemental Material¹⁵) show that the slow relaxing component is unaffected by fields up to 300 G. Combined with the temperature independence of the depolarization rate below 5 K (Fig. 3), this suggests

that quantum rather than thermal fluctuations cause the slow depolarization.

Our magnetization results strongly suggest that the ordering is on the Ir^{4+} sublattice, while the Nd^{3+} moments remain in a paramagnetic state. This ordered state is unusual, as evidenced by the highly damped oscillations and lack of detectable neutron scattering peaks associated with this order. Assuming the muon stopping site(s) are the same for all the *A*-227 materials, the Nd-227 low precession frequency indicates a different magnetic structure than for the insulating Eu, Y, and Yb compounds. We infer from these results two different scenarios: The underlying correlations may produce a “small-moment” system, as observed in UPt_3 or URu_2Si_2 ,¹⁶ or the magnetic order could have a small correlation length and intrinsic texturing. The three-component depolarization described by Eq. (2) combined with the potential presence of strong frustration seem to favor the latter scenario, although such a conclusion is highly speculative given the phenomenological nature of our depolarization function.

In contrast, the onset of magnetism at 120 K has no long-range order, as evidenced by the lack of spontaneous muon precession. In this temperature region, the system is clearly metallic, demonstrating that geometric frustration, if present, is not relieved by a MI transition, unlike the ordering observed around this same temperature in the insulating Eu, Y, and Yb based materials. This ordered phase may be of the spin-glass variety, although our data are also consistent with the prediction of a highly degenerate 2-in/2-out structure which could produce domains with short-range ordering.¹⁷

Our data fail to show that a MI transition occurs in this system, as evidenced by the logarithmic temperature dependence of the resistivity at low temperatures. Also, the variation of the magnetoresistance $\Delta\rho = \rho(H)/\rho(0) - 1$ with magnetization is *negative* and varies linearly with M^2 (inset, Fig. 2), analogous to the Kondo screening observed in $\text{Pr}_2\text{Ir}_2\text{O}_7$, where both the RKKY interaction strength and Kondo temperature are approximately 20 K.⁹ At ambient

pressure, no magnetoresistance has been reported in *A*-227 with a nonmagnetic *A* site; however removing the MI transition of $\text{Eu}_2\text{Ir}_2\text{O}_7$ through the application of high pressure¹⁸ showed that this material exhibits positive magnetoresistance proportional to H^2 , similar to normal metals. We assert that an additional magnetic scattering channel must be present in Nd-227, and it is this process rather than a MI transition that causes the upturn in the resistivity below 8 K. We propose that Nd-227 exhibits a magnetically ordered, metallic ground state, with magnetic order facilitated via RKKY interactions.

In summary, we have studied high quality $\text{Nd}_2\text{Ir}_2\text{O}_7$ samples via magnetization, resistivity, neutron diffraction, and μSR . We find the onset of disordered magnetism at $T = 120$ K, likely arising from the geometric frustration of the Ir^{4+} sublattice. Below $T = 8$ K, long-range magnetic order appears albeit heavily damped; however we find no evidence for a metal-insulator transition, suggesting that the low-temperature magnetic ordering is facilitated via the RKKY interaction. While more detailed studies via both μSR and neutron scattering are required to understand the structure of the magnetically ordered state, our current data demonstrate that the $\text{Nd}_2\text{Ir}_2\text{O}_7$ compound lies just within the metallic phase boundary, potentially within the Dirac semimetal regime, of the proposed topological phase diagram of the pyrochlore iridates.²

We would like to acknowledge very helpful discussions with Ying Ran. This work was supported in part by National Science Foundation Materials World Network Grant No. DMR-0710525 (M.J.G.) and by NSF CAREER Award No. DMR-1056625 (S.D.W.). Muon experiments were performed at the ISIS Muon Facility at the Rutherford Appleton Laboratories (UK) and the Swiss Muon Source at the Paul Scherrer Institute (Switzerland). Part of this work was performed at Oak Ridge National Laboratory High Flux Isotope Reactor, sponsored by the Scientific User Facilities Division, Office of Basic Energy Sciences, US Department of Energy.

¹B. J. Kim, H. Ohsumi, T. Komesu, S. Sakai, T. Morita, H. Takagi, and T. Arima, *Science* **323**, 1329 (2009).

²X. Wan, A. M. Turner, A. Vishwanath, and S. Y. Savrasov, *Phys. Rev. B* **83**, 205101 (2011).

³D. Pesin and L. Balents, *Nat. Phys.* **6**, 376 (2010).

⁴S. Zhao, J. M. Mackie, D. E. MacLaughlin, O. O. Bernal, J. J. Ishikawa, Y. Ohta, and S. Nakatsuji, *Phys. Rev. B* **83**, 180402(R) (2011).

⁵S. M. Disseler, C. Dhital, A. Amato, S. Giblin, C. de la Cruz, S. D. Wilson, and M. J. Graf, [arXiv:1203.6669](https://arxiv.org/abs/1203.6669).

⁶D. Yanagishima and Y. Maeno, *J. Phys. Soc. Jpn.* **70**, 2880 (2001).

⁷N. Taira, M. Wakeshima, and Y. Hinatsu, *J. Phys.: Condens. Matter* **13**, 5527 (2001).

⁸D. E. MacLaughlin, Y. Ohta, Y. Machida, S. Nakatsuji, G. M. Luke, K. Ishida, R. H. Heffner, Lei Shu, and O. O. Bernal, *Physica B* **404**, 667 (2008).

⁹S. Nakatsuji, Y. Machida, Y. Maeno, T. Tayama, T. Sakakibara, J. van Duijn, L. Balicas, J. N. Millican, R. T. Macaluso, and J. Y. Chan, *Phys. Rev. Lett.* **95**, 087204 (2006).

¹⁰K. Matsuhira, M. Wakeshima, R. Nakanishi, T. Yamada, A. Nakamura, W. Kawano, S. Takagi, and Y. Hinatsu, *J. Phys. Soc. Jpn.* **76**, 043706 (2007).

¹¹M. Sakata, T. Kagayama, K. Shimizu, K. Matsuhira, S. Takagi, M. Wakeshima, and Y. Hinatsu, *Phys. Rev. B* **83**, 041102(R) (2011).

¹²J. J. Ishikawa, E. C. T. O'Farrell, and S. Nakatsuji, [arXiv:1203.4182](https://arxiv.org/abs/1203.4182).

¹³K. Tomiyasu, K. Matsuhira, K. Iwasa, M. Watahiki, S. Takagi, M. Wakeshima, Y. Hinatsu, M. Yokoyama, K. Ohoyama, and K. Yamada, *J. Phys. Soc. Jpn.* **81**, 034709 (2012).

¹⁴U. Walter, *J. Phys. Chem Solids* **4**, 401 (1984).

¹⁵See Supplemental Material at <http://link.aps.org/supplemental/10.1103/PhysRevB.85.174441> for detailed results.

¹⁶A. Amato, M. J. Graf, A. de Visser, H. Amitsuka, D. Andreica, and A. Schenck, *J. Phys.: Condens. Matter* **16**, S4403 (2004).

¹⁷A. Ikeda and H. Kawamura, *J. Phys. Soc. Jpn.* **77**, 073707 (2008).

¹⁸F. F. Tafti, J. J. Ishikawa, A. McCollam, S. Nakatsuji, and S. R. Julian, *Phys. Rev. B* **85**, 205104 (2012).